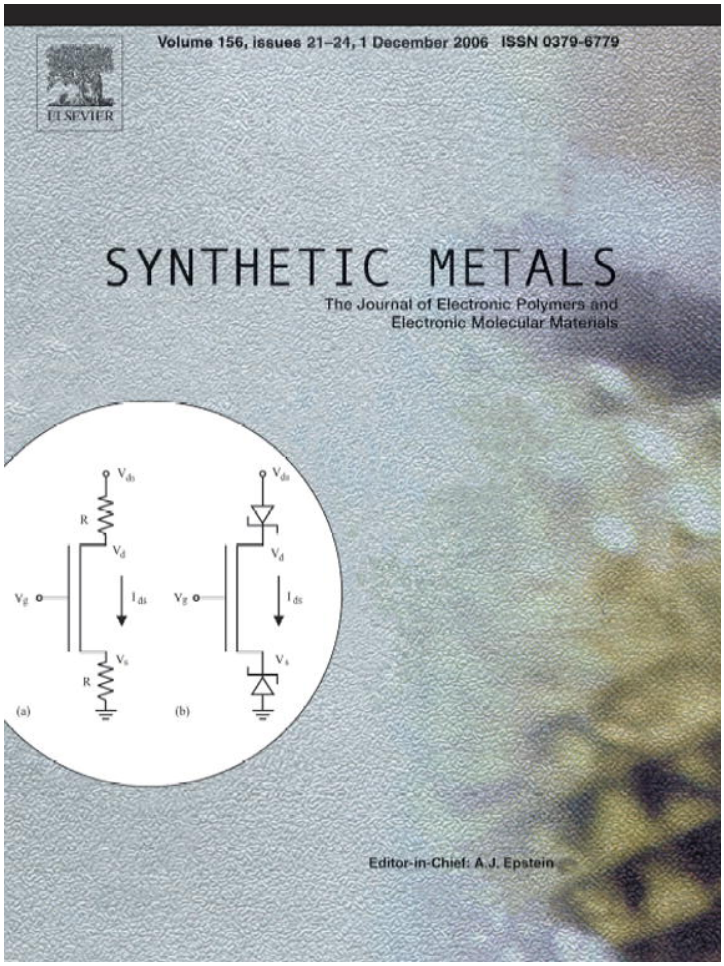

Available online at www.sciencedirect.com
ScienceDirect
Synthetic Metals 156 (2006) 1316–1326
SYNTHETIC METALS
www.elsevier.com/locate/synmet

Modeling electrical characteristics of thin-film field-effect transistors II: Effects of traps and impurities

P. Stallinga*, H.L. Gomes

Universidade do Algarve, FCT, Campus de Gambelas, Faro, Portugal

Received 23 June 2006; accepted 20 September 2006
Available online 20 November 2006

Abstract

Based on a new model for thin-film field-effect transistors, in which the active layer is treated as purely two-dimensional, the effects of impurities on the electrical characteristics are discussed. Localized electronic levels are introduced into the model. It is shown that the presence of traps readily accounts for the non-linearities in the current-voltage curves. Trap states can also explain the temperature dependence of the current and mobility, including the so-called Meyer-Neldel Rule. Finally, transients are qualitatively discussed.

Keywords: Thin-film field effect transistors; Amorphous silicon; Organic semiconductors; Traps

1. Introduction

In the first part of this contribution, a two-dimensional model for trap-free thin-film field-effect transistors based on intrinsic materials was derived [1]. Differential equations were found where the current at each point in space is proportional to the induced charge density, the local field and the mobility, which was considered constant. The solution of this set of differential equations was *I–V* curves and transfer curves very similar to those of MOS-FETs.

The technological knowledge of inorganic materials has reached a level in which crystals can be made of them with near absolute purity and crystallinity. Modern materials, such as most organics, do not reach that level, yet, and a high density of deep levels is to be expected. Another possible source for traps is that thin-film layers in TFTs are nearly always grown on top of non-lattice-matching other materials. The lattice mismatch causes the layer to be amorphous with an unavoidable high density of defects. Especially at the interface – the most critical part of the device – deep levels from dangling bonds can be present, either in the insulator or in the active material. In silicon based devices, many years of efforts devised ways to reduce the density of these "surface states" to negligible values. For organic based devices such "cleaning up" processes are still in their infancy. For instance, recently, Chua et al. have made the observation that n-type behavior in organic-based transistors has been hampered by a high density of electron traps caused by unpassivated defects in the surface of the silicon oxide layer [2]. In this part we will discuss the effects on the *I–V* and transfer curves of intentional (doping) and unintentional introduction of electronic levels. First, the general effects of trapping on the threshold voltage are presented. Then the effects of doping and traps on *I–V* curves and transfer curves are discussed. The new deep levels also change the dependence of the current on temperature as is discussed next, including the so-called Meyer-Neldel Rule, where the activation energy of current depends on the bias conditions. Finally, transients are briefly discussed.

Unless specified otherwise, the linear mode of operation is assumed, with a drain-source bias so small that the density of charge is constant along the entire channel and the approximation

$$I_{\mathrm{ds}} = qW\frac{V_{\mathrm{ds}}}{L}\mu p(V_{\mathrm{g}}) \tag{1}$$

can be made. The bias dependence of the current then becomes

$$\frac{\partial I_{\mathrm{ds}}}{\partial V_{\mathrm{g}}} = \frac{\partial I_{\mathrm{ds}}}{\partial p}\frac{\partial p}{\partial V_{\mathrm{g}}} = \frac{W}{L}\mu V_{\mathrm{ds}} q\frac{\partial p(V_{\mathrm{g}})}{\partial V_{\mathrm{g}}} \tag{2}$$

* Corresponding author. Tel.: +351 969541198; fax: +351 289800030.
E-mail address: pjotr@ualg.pt (P. Stallinga).

0379-6779/$ – see front matter © 2006 Elsevier B.V. All rights reserved.
doi:10.1016/j.synthmet.2006.09.008

and the as-measured mobility of Eq. (4) of Ref. [1] is

$$\mu_{\mathrm{FET}} = -\frac{q\mu}{C_{\mathrm{ox}}}\frac{\partial p(V_{\mathrm{g}})}{\partial V_{\mathrm{g}}} \tag{3}$$

or, in other words, the as-measured mobility is proportional to the intrinsic mobility μ and the dependence of the free carrier density on the gate bias. This dependence is not necessarily linear, as we will show, and a bias-dependent as-measured mobility μ_{FET} can result.

2. Threshold voltage

For an MOS-FET, it can be demonstrated that the threshold voltage in an inversion p-channel FET is $V_{\mathrm{t}} = 2\psi_{\mathrm{B}} + \sqrt{2\varepsilon q N_{\mathrm{D}} 2\psi_{\mathrm{B}}}/C_{\mathrm{ox}}$, with N_{D} the donor concentration, and ψ_{B} the distance from mid-gap to the bulk Fermi level ($2\psi_{\mathrm{B}}$ is the distance the Fermi level should be shifted to create an equal density of charges of opposing sign as compared to the bulk) [3]. The same model predicts a sub-threshold current exponentially depending on the gate bias, defining a sub-threshold swing $S \equiv \mathrm{d}V_{\mathrm{g}}/\mathrm{d}(\log\ I_{\mathrm{ds}})$ [3]. Using the same reasoning, the threshold voltage in an accumulation type FET is zero (V_{t} is the voltage needed to create a charge density equal to the one in the bulk, this time not of opposite sign; by definition zero). Sometimes, in literature, the somewhat arbitrary definition is used that the charge should have doubled at threshold [4]. Before continuing the discussion of the threshold voltage, it is important to present the correct procedure for extracting the threshold voltage from experimental data.

The threshold voltage can be found by fitting a straight line in a transfer curve in the linear region and extrapolating to zero current. However, extracting the threshold voltage in this way is not always easy. Fig. 1 shows an experimentally obtained transfer curve in the linear region for an FET based on T6. From this curve it is clear that the slope (and thus the mobility via Eq. (3)) and the threshold voltage found by extrapolation to $I_{\mathrm{ds}} = 0$ depend on the point of the curve used; both μ and V_{t} depend on V_{g}. The awkward situation arises in which both mobility and threshold voltage can depend on the bias point considered. Further on, in the section on the transfer curves we will show how the mobility can depend strongly on the gate bias, resulting in non-linear, power-law curves. For now, it suffices to say that the correct procedure for extracting the threshold voltage is first linearizing the curves by taking the nth root of the current. The threshold voltage can then be found by extrapolation as before. Fig. 1 b shows such a linearized curve and the threshold voltage in this case is zero.

The observed threshold voltage can deviate from zero in cases when the gate-induced charge is not mobile. In that case, at zero bias there is charge (ρ), but no current. The total charge is trapped charge (p_{t}) plus free charge (p), thus $q(p + p_{\mathrm{t}}) = C_{\mathrm{ox}} V_{\mathrm{g}}$ and this defines the threshold voltage as

$$V_{\mathrm{t}} = \frac{-qp_{\mathrm{t}}}{C_{\mathrm{ox}}} \tag{4}$$

It is important to note that in an accumulation type FET there is no direct link between the threshold voltage and acceptor or donor concentrations, though V_{t} might be limited by the availability of traps.

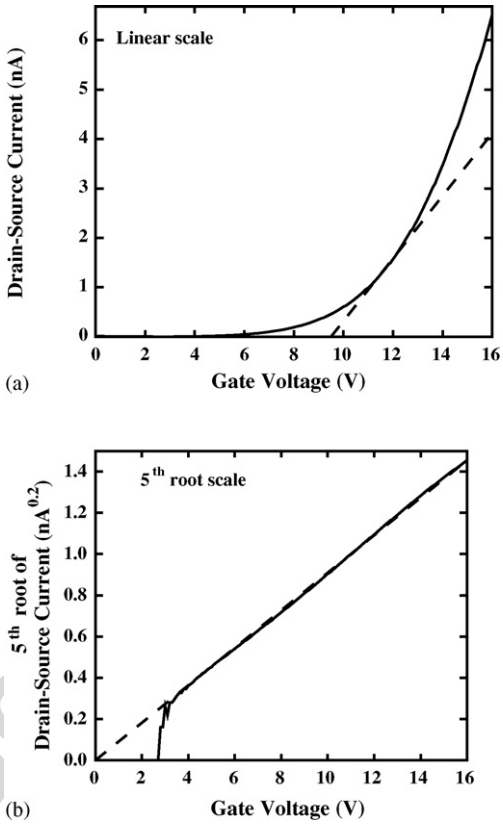

Fig. 1. (a) Experimental transfer curve for an FET based on T6 showing power-law dependence in the linear region. The as-measured mobility (Eq. (3)) and threshold voltage depend on the bias point of the curve considered. The dashed line shows an example at $V_{\mathrm{g}} = 12\,\mathrm{V}$ yielding $V_{\mathrm{t}} = 9.5\,\mathrm{V}$ and $\mu = 2 \times 10^{-5}\,\mathrm{cm^2/Vs}$ (b) The same transfer curve but linearized by taking the fifth root of the current. The threshold voltage V_{t} found by extrapolation is zero.

An effect known as "stressing" is a phenomenon that the threshold voltage is slowly and continuously shifting upon application of the gate bias. In view of the model described here, this can be attributed to trapping of free charge on deep localized states. A positive threshold voltage can equally easily be achieved by trapping electrons. The trapped electrons [2] are then compensated by free holes and a channel exists even without bias, $p - n_{\mathrm{t}} = 0$, and $V_{\mathrm{t}} = qn_{\mathrm{t}}/C_{\mathrm{ox}}$. This results in a "normally-on" FET. Fig. 2 shows an experimental example of how the gate bias can cause positive as well as negative threshold voltages, depending on the sign of the bias. Thus confirming that both holes and electrons can be trapped.

Fig. 3 demonstrates the amphoteric nature of trapping in a typical organic semiconductor, sexithiophene (T6). In this thermally stimulated current (TSC) experiment, the device is cooled down with a gate bias switched on (with drain and source interconnected and grounded). Depending on the sign of the bias, electrons ($V_{\mathrm{g}} > 0$) or holes ($V_{\mathrm{g}} < 0$) are induced in the channel and are available for trapping. At low temperatures the gate bias is removed and the current coming out of the source and drain monitored with the current meter while the temperature is ramped up. When charges are released from

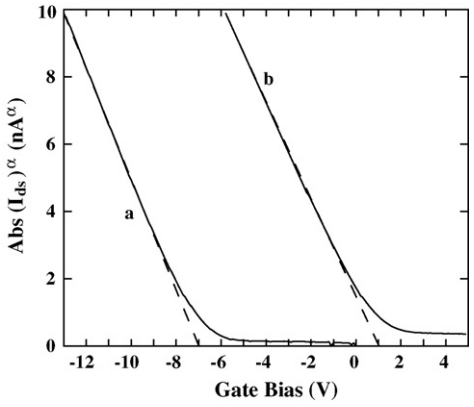

Fig. 2. Experimental transfer curves for a T6 TFT. Upon prolonged application of a gate bias, the same device can be programmed to have large negative (a) or positive (b) threshold voltage V_t. The former is achieved by trapping the free holes induced by a negative gate bias, whereas the latter is achieved by trapping the free electrons induced by a positive gate bias. Curves are linearized by the procedure described in the text.

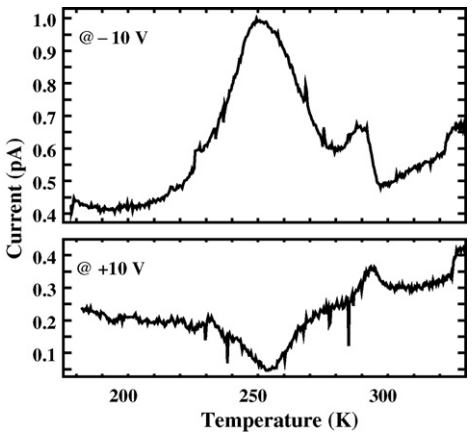

Fig. 3. Experimental thermally-stimulated currents (TSC) at zero bias in a device of sexithiophene (T6), cooled down at two different biases ($V_g = -10$ V, top and +10 V, bottom). This shows the amphoteric trapping character of the material, being able to trap both holes and electrons. Scanning speeds 44 and 41 mK/s, respectively.

the traps, they contribute to an external current that disappears again once the traps are empty. The figure shows both signs of currents indicating that both types of carriers can be trapped. For the set-up used for this particular measurement, a positive peak indicates positive charge emitted from traps and negative peak negative charge. The same conclusion as for the threshold voltage of Fig. 2, can be drawn for the TSC measurements, namely a more efficient hole trapping compared to electron trapping.

3. Effect of traps on the *I–V* curves

Non-linearities are often observed in *I–V* curves. They can be described as supra-linear close to the origin, and are often attributed to the effects of the contacts. As we have shown in earlier sections of this work, this in not an adequate physical picture. We will now discuss how an abundant trap can readily explain these anomalous *I–V* curves.

A Poole and Frenkel approach shows how the current, and thus the effective mobility ($\mu \propto I_{ds}/V_{ds}$), of a trap-ridden material can depend on the temperature and electrical field [3,5]:

$$\mu_{PF} = \mu_0 \exp\left[-\frac{(E_T - E_V) - q\sqrt{q|E_x|/\pi\varepsilon}}{kT}\right], \tag{5}$$

with μ_0 the free carrier mobility, $E_T - E_V$ the discrete trap depth, $E_x = dV(x)/dx$ the in-plane electric field, ε the permittivity of the material and q the elementary charge. The effect on the temperature dependence of the current will be described further on. Here we discuss the field effect. Including a field dependent mobility into the model, the differential equations for TFTs now become

$$\begin{aligned} I_x(x) &= Wqp(x)\mu(x)\frac{dV(x)}{dx} \\ p(x) &= \frac{C_{ox}[V_g - V_t - V(x)]}{q} \\ \mu(x) &= \mu_{00}\exp\left(\frac{a}{kT}\sqrt{|dV(x)/dx|}\right), \end{aligned} \tag{6}$$

where the same boundary conditions apply as before ($V(0) = 0$, $V(L) = V_{ds}$ and $I_x(x) = I_{ds}$) and $\mu_{00} = \mu_0 \exp[-(E_T - E_V)/kT]$ depends on the temperature and the trap depth and $a = \sqrt{q^3/\pi\varepsilon}$ is a constant that depends only on the permittivity of the material (ε). The above equations do not have a simple analytical solution, however, they are not difficult to solve numerically. Fig. 4 shows simulations of the *I–V* curves for different temperatures (see Table 1).

The curves are clearly supra-linear for small V_{ds}, especially for lower temperatures, because a larger portion of the charges is trapped, whereas for higher temperatures the charges are excited to the mobile band and the mobility approaches μ_0, independent of field. It is also predicted that the non-linearities become more pronounced when the channel length is reduced. This, because the factor in the exponent of Eq. (6) scales with the inverse of the channel length and takes an increasingly important role. As to the effect on the shapes of the curves, it can be said that the effect of reducing the channel length is equal to lowering the temperature. This will be technologically important when the devices are reduced to nano-scale dimensions. Severe non linearities can be expected when abundant traps are present.

In conclusion, non-linearities are readily explained in the framework of traps by assuming a field-assisted thermal excitation from these deep levels, as proposed by Poole and Frenkel.

Table 1
Simulation parameters used in this work (unless otherwise specified)

Parameter	Value	Unit
N_V	1.04×10^{16}	m^{-2}
C_{ox}	160	$\mu F/m^2$
V_{ds}	−0.1	V
g_{T0}	10^{18}	m^{-2}/eV
T_2	800	K
W	1	cm
L	10	μm
μ_0	3	cm^2/Vs
E_g	1.12	eV

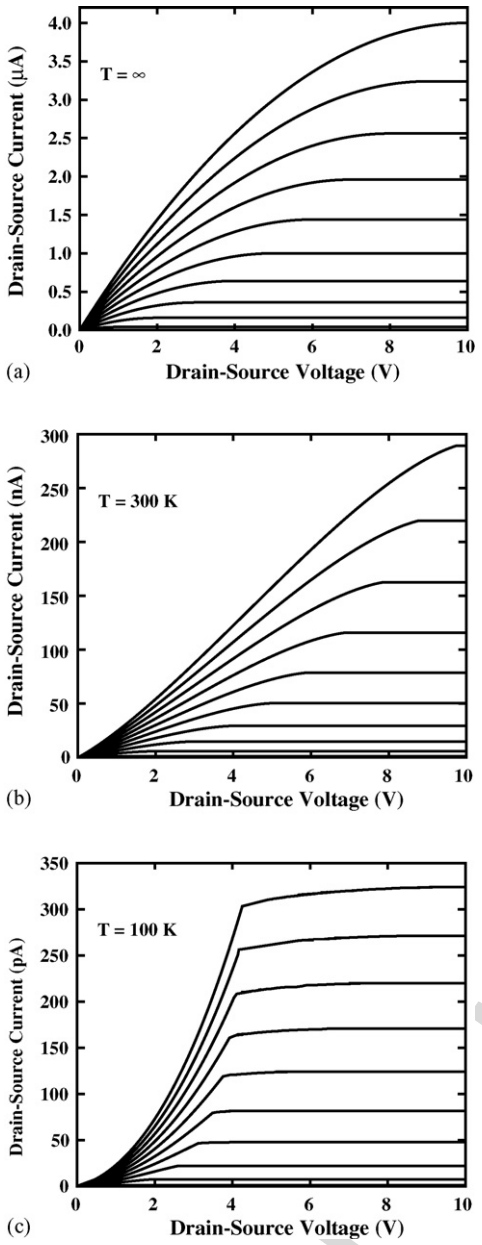

Fig. 4. Simulations of *I–V* curves for field-dependent mobility as described by Poole and Frenkel for temperatures as indicated. Gate bias ranging from 1 to 10 V. Parameters as in Table 1 and $E_T = 100$ meV and $\varepsilon = 5\varepsilon_0$. For small field dependence (infinite temperature), the familiar FET curves emerge. However, for larger field dependence, the curves become pronouncedly concave (supra-linear).

The model described above has, apart from the scaling parameter E_T, only one adjustable parameter, namely the permittivity of the material, ε. For the simulations in Fig. 4, an ε equal to $5\varepsilon_0$ was assumed; a reasonable value. For lower ε the effects are more pronounced. As shown before, in standard theory the currents are independent of the ratio *W*:*L*. When Poole-Frenkel conduction is important, this is no longer true, since the current depends non-linearly on *L*. Severe short-channel effects thus result.

As a final remark, note that the field used in the calculation is only the in-plane field E_x. This is because the perpendicular field E_y is shielded by the build-up of charges. Since there is no current in this direction, the total field is necessarily zero: $0 = J_y = qp\mu E_y$.

4. Doping, defects and impurities and their effect on the transfer curves

For a TFT, without contact effects, in the linear region the currents depend linearly on the gate-bias (and drain-bias). The assumption was that the induced free charge in the channel is linearly depending on the gate bias, because all the charge induced by the gate is free charge. For traditional materials, viz. Si or GaAs, this is a valid assumption because the acceptors and donors introduce shallow levels, which are consequently all ionized at all operational temperatures. Any additional charge induced by the gate is necessarily free charge. This then predicts currents rather independent of temperature (since the dependence of the mobility on the temperature is small) and linearly depending on bias. Yet, the currents of organic TFTs are normally strongly temperature dependent and often bias dependent [6–10]. In this section we will discuss the various reasons that might cause such observation, ranging from shallow and deep acceptors to traps and show that only the latter can adequately explain the observations.

As a first suspect for this behavior we try deep acceptors. Acceptors are impurities in the material that can accept an electron from the valence band and can thus be either neutral or negatively charged. In the materials used in modern TFTs, especially organic materials, the acceptor and donor states can be very deep and abundant. Fig. 5 shows a graphical method of finding the Fermi level and charge densities following the method presented by Sze [3] of plotting all negative and all positive charge in separate curves. The Fermi level is then found by the crossing point of the curves, representing charge neutrality. As demonstrated by Fig. 5, for deep abundant acceptors N_X, while resulting at room temperature in a free-hole density p equal to the case of less-abundant shallow acceptors N_A, this free charge density depends on the temperature. When the temperature is raised, the slopes of all the slanted curves are reduced (proportional to $1/kT$). This moves the charge-neutrality point (•) up, indicating an increase of p and $N_X{}^-$ at a constant E_F; electrons are thermally excited from the valence band into the traps (or holes from the traps into the valence band). On the contrary, for shallow acceptors (solid curve) this point moves sideways, indicating a change in Fermi level, but no change in p or $N_A{}^-$.

The consequence of a huge density of such deep acceptors is that the assumption that all induced charge is free charge is no longer valid. Whereas the total induced charge ρ in the channel is still equal to $-C_{ox}V_g$, this is divided over the free charge $p - n$ and immobile charge $N_X{}^-$ and each (can) depend on the gate bias differently. Only the free charge contributes to current. Imagine a situation with a deep acceptor density so high that at room temperature they are not completely filled, as in Fig. 5. When a negative gate bias is applied, the Fermi level E_F will shift down $-\delta E_F$ in such a way as to increase the total charge density. For the Fermi level far away ($\gtrsim 3$ kT) from the deep level the distributions follow (using the Boltzmann distribution

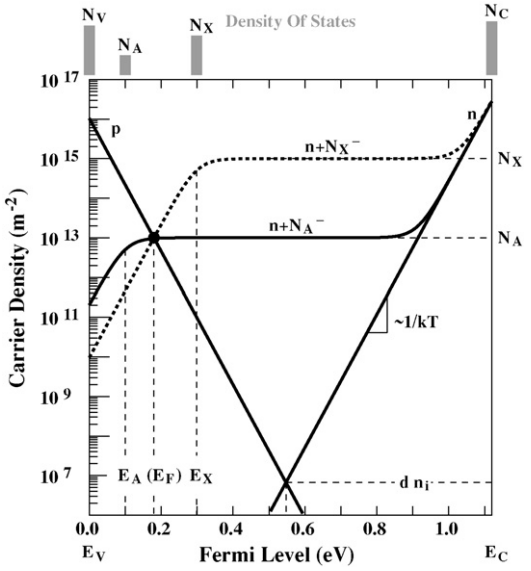

Fig. 5. Graphical method of finding the Fermi level. The hole density p, electron density n and ionized acceptor density $N_A{}^-$ depend on the position of the Fermi level, E_F. Demanding charge neutrality yields the value of E_F and the zero-bias free charge density p_0 as the crossing point of the curves for positive and negative charge, as indicated by the full circle (•). The same Fermi level (and free hole density) found for a fully ionized acceptor at E_A with density N_A can be found for a partially ionized deep acceptor level at E_X with abundance N_X. In the latter case, the free hole density and ionized acceptor density (but not the Fermi level) depend on the temperature. In the former case the Fermi level (but not the free hole density or ionized acceptor density) depends on the temperature. Above the figure, a schematic representation of the DOS is given. Units of densities are all converted to 1/m^2 via the channel thickness d (assumed to be 1 nm).

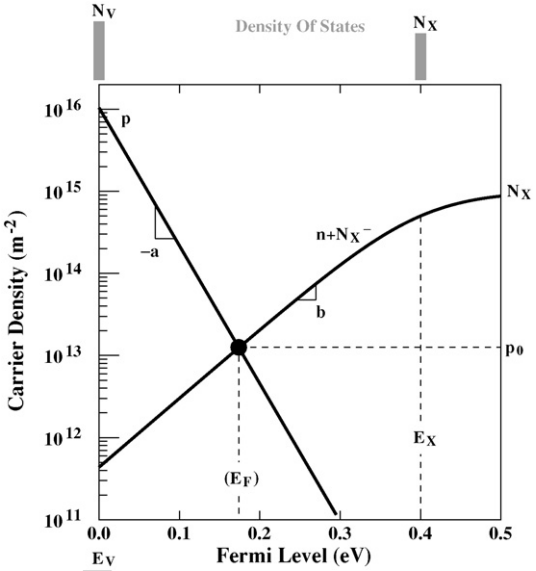

Fig. 6. Graphical representation of the density of charge when the curves of positive and negative charge have different slopes. As demonstrated in the text, this still results in linear transfer curves.

function)

$$p = N_V \exp\left[\frac{(E_V - E_F)}{kT}\right] \tag{7}$$

$$N_X{}^- = N_X \exp\left[\frac{(E_F - E_X)}{kT}\right] \tag{8}$$

Considering that the total charge is

$$q(N_X{}^- - p) = C_{ox} V_g \tag{9}$$

the solution is that the as-measured mobility (Eq. (3)), that is proportional to the derivative of free-carrier concentration, is

$$\mu_{FET} \propto -\frac{dp}{dV_g} = \frac{C_{ox}}{q}\frac{1}{(p_{01}/p)^2 + 1} \tag{10}$$

with p_{01} the zero-bias free-hole concentration,

$$p_{01} = \sqrt{N_V N_X}\exp\left[\frac{(E_V - E_X)}{2kT}\right] \tag{11}$$

When the channel is formed, $p \gg p_{01}$ and the as-measured mobility is independent of gate bias, even when an appreciable amount of deep states N_X is present; the transfer curves are linear. Introducing a second deep level does not change this. As long as the slope in the curves of both p and $n + N_X{}^-$ is $\pm 1/kT$, there will be no dependence of the mobility on V_g.

This might change when the Fermi level is at, or in the vicinity of, the trap level and, locally, the slopes are different. This situation will now be investigated. When E_F is close to E_X Eq. (8) is replaced by the full Fermi-Dirac distribution function instead of the Boltzmann approximation used above:

$$N_X{}^- = N_X \frac{1}{1 + \exp[(E_X - E_F)/kT]} \tag{8'}$$

which yields a complex solution when substituted into Eq. (9). It is more interesting to analyze a general case when the slopes of p and $N_X{}^-$, locally at the Fermi level, are different. Imagine the slope of p to be $-a$, and the slope of $N_X{}^-$ to be b, with a and b parameters that can still depend on temperature. Fig. 6 shows this graphically. As long as the densities p and $N_X{}^-$ are high, (when the channel is open), the Fermi level does not move much upon changes of bias and a and b can be considered constant over a large voltage range. In this case, the above equations are replaced by

$$p = N_V \exp[-a(E_F - E_V)] \tag{7''}$$

$$N_X{}^- = N_X \exp[b(E_F - E_X)] \tag{8''}$$

The solution of the equations above is that (ignoring the tiny contribution of n)

$$p_{02}\left(\frac{p_{02}}{p}\right)^{b/a} - p = \frac{C_{ox} V_g}{q} \tag{12}$$

with the p_{02} the zero-bias hole concentration,

$$p_{02} = N_X{}^{a/(a+b)} N_V^{b/(a+b)} \exp\left[\frac{ab}{a+b}(E_V - E_X)\right] \tag{13}$$

For equal slopes (for example $a = b = 1/kT$) this reduces to the earlier found mobility of Eqs. (10) and (11). In any case, for $p \gg p_{02}$ the first term of Eq. (12) is negligible and linear transfer curves and bias-independent mobility result. Thus we conclude that shallow or deep acceptors are not able to explain a bias-dependent mobility, even when they are not discrete.

Instead of deep acceptors, the material might have abundant traps N_T. Traps differ from acceptors in that they can be neutral

(N_T^0) or positively charged (N_T^+) and can thus capture free holes. We will now show that such traps can result in a bias-dependent mobility.

First we will analyze a case of a discrete trap. In this case, the density of free holes follows Eq. (7) and the density of charged traps is

$$N_T^+ = N_T \exp\left[\frac{(E_T - E_F)}{kT}\right] \tag{14}$$

Once more, the charge induced by the gate is the difference in positive and negative charge, but the contribution of n is minute. Thus the total induced charge becomes

$$p + N_T^+ = \frac{-C_{ox} V_g}{q} \tag{15}$$

or

$$p\left(1 + \frac{N_T}{N_V}\exp\left[\frac{(E_T - E_V)}{kT}\right]\right) = \frac{-C_{ox} V_g}{q} \tag{16}$$

As can be seen, this results in a reduced as-measured mobility (defined in Eq. (3)). Especially when the density of charged traps is much higher than free holes, the as-measured mobility can be much smaller than the intrinsic mobility. Moreover, the mobility becomes temperature dependent, as will be discussed later. At this stage, however, the conclusion is that a discrete trap results in a gate-bias-independent mobility, since p depends linearly on V_g. For less abundant traps, they can become exhausted for increased biases. When the bias makes the Fermi level cross the trap level, the approximation of Eq. (14) becomes invalid. In this case, the contribution of $N_T{}^+$ in Eq. (15) becomes negligible and the device returns to the trap-free situation, with a noticeable increase in as-measured mobility.

We will now look at a more generalized situation. Imagine a situation, with concentrations of free holes p, free electrons n and trapped charge $p_t = N_T{}^+$ depending on the Fermi level in a different way

$$p = N_V \exp[-a(E_F - E_V)] \tag{17}$$

$$N_T{}^+ = N_0(T)\exp[-c(E_F - E_V)] \tag{18}$$

as in Fig. 7. In this, N_0 is a function of T but not of E_F. Substituting this into the charge-bias relation of Eq. (15) results in

$$p + p_{03}\left(\frac{p}{p_{03}}\right)^{c/a} = \frac{-C_{ox} V_g}{q} \tag{19}$$

with p_{03} equal to

$$p_{03} = N_0^{a/(a-c)} N_V^{-c/(a-c)} \tag{20}$$

The interesting situation can exist when the trapped charge (second term in Eq. (19)) is much larger than the free charge (see Fig. 7). In that case, the as-measured mobility becomes strongly bias dependent:

$$p = \left(\frac{-C_{ox} V_g}{q}\right)^{a/c} N_V N_0^{-a/c} \tag{21}$$

The as-measured mobility of Eq. (3), being proportional to the derivative of $p(V_g)$, becomes

$$\mu_{FET} = \mu_0 \frac{a}{c}\left(\frac{-C_{ox} V_g}{q}\right)^{a/c-1} N_V N_0^{-a/c} \tag{22}$$

The interesting question now is: How can the slope of the density of trapped charge $N_T{}^+$ or free charge p in Fig. 7 be different than $1/kT$? Inspired by the work of Shur and Hack [11], we try a density of states (DOS) function exponentially decaying in energy

$$N_T(E) = g_{T0}\exp\left(\frac{E_V - E}{kT_2}\right) \tag{23}$$

with g_{T0} the density of states at $E = E_V$ and T_2 the decay rate, parameters that describe the distribution. The dependence of $N_T{}^+$ on the position of the Fermi level then becomes

$$N_T{}^+(E_F) = \int_{-\infty}^{\infty} N_T(E)[1 - f(E - E_F)]dE \tag{24}$$

with f the Fermi-Dirac distribution function,

$$f(E - E_F) = \frac{1}{1 + \exp[(E - E_F)/kT]} \tag{25}$$

The integral of Eq. (24) converges when $T < T_2$. To a good approximation, the solution can be found by dividing the integral into two parts, see Fig. 8. In the first part, below E_F, the slope is $1/kT - 1/kT_2$ as a result of the difference of slopes in N_T and the exponential approximation for $1 - f$. Above E_F, $1 - f$ is considered unity and the resulting slope is $1/kT_2$. With this help, it can easily be shown that the integral is equal to

$$N_T{}^+(E_F) = N_0(T)\exp\left(\frac{E_V - E_F}{kT_2}\right) \tag{26}$$

where

$$N_0(T) = \alpha(T) g_{T0}\frac{k^2 T_2^2}{kT_2 - kT} \tag{27}$$

with $\alpha(T)$ a slowly varying, dimensionless function depending only on the temperature. $\alpha(T)$ is an ad-hoc correction factor that compensates for the error of integration; compare the rounded distribution of $N_T{}^+$ of Fig. 8 and the triangular integration described above. Numerical simulations show that $\alpha(T)$ oscillates between 1 and 0.8 in the temperature range 0 - T_2, see Fig. 9). This makes N_0 essentially temperature independent for T not very close to T_2. For $T \geq T_2$ the integral diverges.

Comparing Eq. (26) with Eq. (18) we see that

$$c = \frac{1}{kT_2} \tag{28}$$

Assuming a normal distribution of band states (implying $a = 1/kT$), we find a bias and temperature dependent mobility of Eq. (22)

$$\mu_{FET} \propto (-V_g)^{T_2/T - 1} \tag{29}$$

which is similar, but not equal, to the result found by Shur and Hack [11]. The differences will be discussed further on.

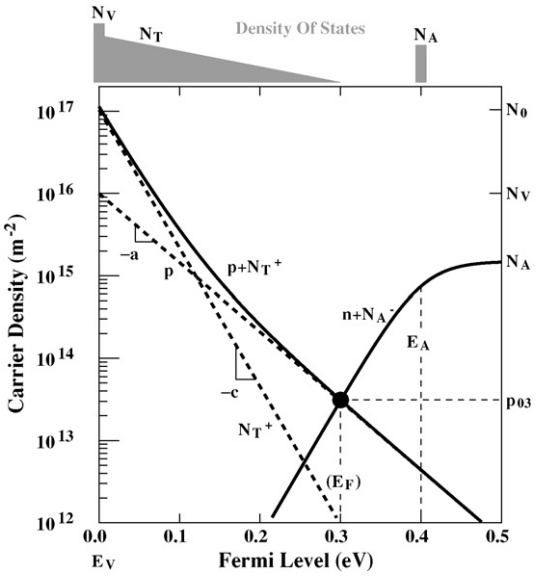

Fig. 7. Graphical representation of the density of charge when there are two types of states capable of storing positive charge, valence band states N_V storing free holes p and trap states N_T storing immobile charge p_t. When they have a different Fermi-level dependence, the result is a gate-bias dependent mobility, as described in the text.

Finally, when also the conduction states of the valence band are distributed in energy, in so-called band-tail states,

$$N_V(E) = g_{V0} \exp\left(\frac{E_V - E}{kT_1}\right) \tag{30}$$

with g_{V0} the density-of-states at $E = E_V$, similar argumentation will result in a bias dependent - but nearly temperature independent - mobility; $a = 1/kT_1$ and the gate-bias dependence becomes

$$\mu_{FET} \propto (-V_g)^{T_2/T_1 - 1} \tag{31}$$

Interesting in view of this are the results of a particular T6 TFT presented by us in an earlier work of a bias-dependent mobility, $\mu_{FET} \propto V_g^5$ for all temperatures measured [6].

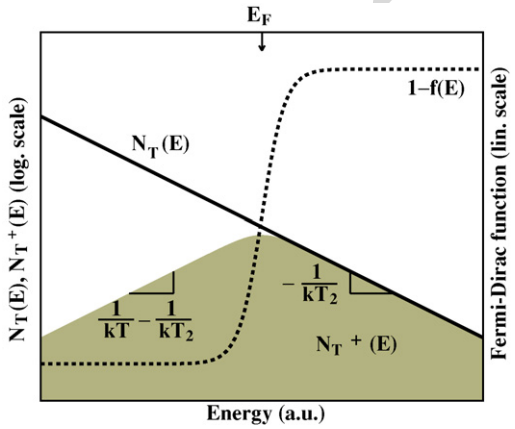

Fig. 8. Graphical schematic of the distribution in energy of trap states $N_T(E)$ (solid line) and charged trap states N_T^+ (shaded area). The latter is a result of a multiplication of the former by the Fermi-Dirac function $1 - f(E)$ (dashed line). This shows that the total trapped charge N_T^+ as a function of Fermi level, see the integral of Eq. (24), can easily be approximated by dividing the integral into two parts.

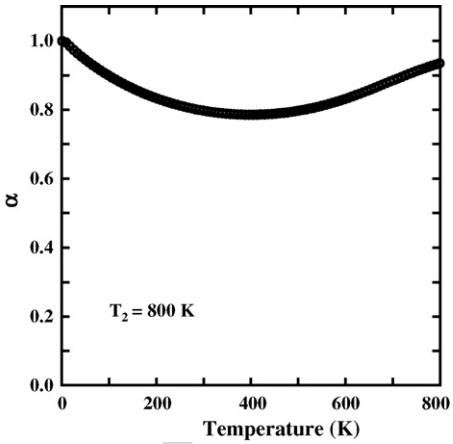

Fig. 9. The ad-hoc correction factor α as a function of temperature, calculated numerically. α is a slowly varying function of T and its contribution to the calculation is minimal. For the coming calculations, α is approximated by a third-order polynomial (solid line).

The relevant idea to retain is that the field-effect mobility is gate-bias dependent when the ratio of trapped charge to free charge density is relatively high.

5. Temperature dependence and the Meyer-Neldel Rule

In most materials, the mobility is only weakly temperature dependent ($\mu \propto T^\alpha$, with α depending on the limiting factor, ranging from $-3/2$ for acoustic phonons, to 1/2 for optical-phonon scattering) [3]. Moreover, since shallow donors or acceptors can be considered fully ionized at all relevant temperatures, the currents, and hence the effective mobilities, according to Eq. (3) are rather temperature independent. As discussed before, in the case of deep acceptors, not all are ionized at room temperature. The free-carrier density and bulk conductivity of the material then depends exponentially on the temperature; Arrhenius plots of the logarithm of conductivity or resistivity versus reciprocal temperature are straight lines.

The effects on the FET currents are different. For discrete deep acceptors, see Fig. 5, it was shown that, when the induced charge is much larger than the zero-bias free hole concentration, this induced charge is only free holes. Therefore, the transfer curves are linear – the mobility is constant (Eq. (10)) – and the currents are independent of temperature. The same reasoning can be applied to an acceptor distributed in energy. In case of acceptors, even when not completely ionized, the currents are independent of temperature, because the induced charge is predominantly free charge.

The conclusion is that even in the presence of shallow or deep acceptors, the transport mechanism is still dominated by the free charge and the currents are independent of temperature. A temperature-dependent current and mobility can only be explained in the framework of traps, as we will show now.

When the density of traps is high, Eq. (16) reduces to

$$p = \frac{C_{ox} V_g}{q} \frac{N_V}{N_T} \exp\left(-\frac{E_T - E_V}{kT}\right) \tag{32}$$

Since the activation energy is defined as the slope of an Arrhenius plot ($\ln(I_{ds})$ versus $1/kT$), and, using the linear relation of I_{ds} and p of Eq. (1), we get a bias-independent activation energy of

$$E_a \equiv -\frac{\mathrm{d}\,\ln(I_{ds})}{\mathrm{d}(1/kT)} = E_T - E_V \tag{33}$$

This is exactly the Poole-Frenkel activation energy if we remember that the effective trap depth can further be modulated by a field.

More general distributions can result in a bias-dependent activation energy. Using Eqs. (19) and (20), with the definition of N_0 as in Eq. (27) ($c = 1/kT_2$) for trap states and conduction states exponentially distributed in energy:

$$p = \left(\frac{-C_{ox}V_g}{q}\right)^{a/c} N_0^{-a/c} N_V \tag{34}$$

For trap states exponentially distributed in energy, as described before, $c = 1/kT_2$, and normal band states, $a = 1/kT$, we find an activation energy for the current that depends on the gate bias:

$$E_a = kT_2 \ln(N_0) - kT_2 \ln\left(\frac{-C_{ox}V_g}{q}\right) \tag{35}$$

where N_0 is only moderately dependent on T and can be considered constant when T not close to T_2, resulting in linear Arrhenius plots.

The Meyer-Neldel Rule [12] is an observation, originally without an explanation, that the activation energy of a process – for instance current or carrier mobility – depends on a parameter and that there exists a temperature, known as the iso-kinetic temperature T_{MN} where the dependence disappears. Many observations of this are reported in literature [13–23]. Looking at our results, we can see that the current and the mobility can depend on the gate-bias when they are controlled by a huge density of traps, distributed in energy. Eq. (34) shows the temperature dependence of the free charge density (and the current through the relation of Eq. (1)). Fig. 10 shows a simulation of these currents for $a = 1/kT$ and $c = 1/kT_2$ with $T_2 = 800$ K. Eq. (34), remembering that $a/c = T_2/T$, predicts an infinite iso-kinetic temperature, $T_{MN} = \infty$. Upon closer scrutiny, analyzing the Fig. 10 reveals that the temperature dependent terms in N_0 make the iso-kinetic temperature shift slightly. Note also a dramatic drop in current when the temperature approaches T_2. The slope in a plot of the as-measured activation energy versus bias is kT_2, see the inset of Fig. 10 and this is thus the most accurate way of determining T_2.

At the same time, because the mobility is proportional to the derivative of the free-carrier concentration (Eq. (3)), the iso-kinetic temperature for mobility is equal to $T_{MN} = T_2$. Analyzing Eq. (22) it can be seen that the activation energy of mobility is equal to the one found for current, see Eq. (35). Because of the added factor a/c ($= T_2/T$), with respect to the Arrhenius plot of currents, the non-linearities increase and the experimental curves do not converge neatly to one point, see Fig. 11. Experimentally, because of various sources of noise and instrumental distortions, it will be difficult to determine this non-perfect converging. In any case, a better procedure would be to plot the logarithm of μT versus $1/T$. This makes the curves more linear.

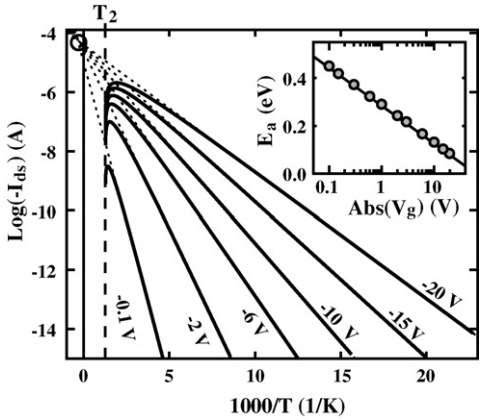

Fig. 10. Arrhenius plots of current for various gate biases as indicated. The iso-kinetic temperature, T_{MN}, where the current is independent of bias, can be found by extrapolation and is close to infinity (○). The vertical dashed line indicates $T = T_2$. When approaching this temperature, the currents drop dramatically because of the temperature dependence of N_0. The Arrhenius plots are linear over a wide range of temperatures, allowing for the determination of the as-measured mobility via the slopes of the curves (dashed lines). The inset shows E_a as a function of bias, with the solid line a simulation of Eq. (35). The parameters of the simulation are given in Table 1.

Finally, when also the mobile states are distributed in energy, in so-called band-tail states, then $a = 1/kT_1$ and the current and mobility become nearly temperature independent. In that case, the mobility is proportional to V_g^{γ} with $\gamma = T_2/T_1 - 1$ independent of temperature. Fig. 12 shows a simulation of the transfer curves for various temperatures in a logarithmic and linear scale. The inset shows a possible DOS resulting in such behavior. The transfer curves are indeed very similar to what we observed in a TFT of sexithiophene [6].

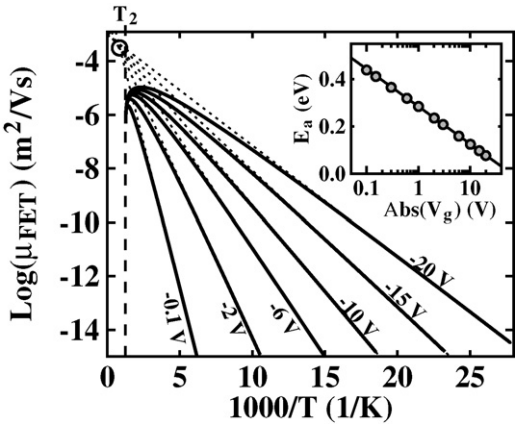

Fig. 11. Arrhenius plots of mobility for various gate biases. The iso-kinetic temperature, T_{MN}, where the mobility is independent of bias, is close to T_2 and is indicated with ○. The vertical dashed line indicates $T = T_2$. The Arrhenius plots are linear over a wide range of temperatures, allowing for the determination of the as-measured mobility via the slopes of the curves (dashed lines). The inset shows E_a as a function of bias, with the solid line a simulation of Eq. (35). The parameters of the simulation are given in Table 1.

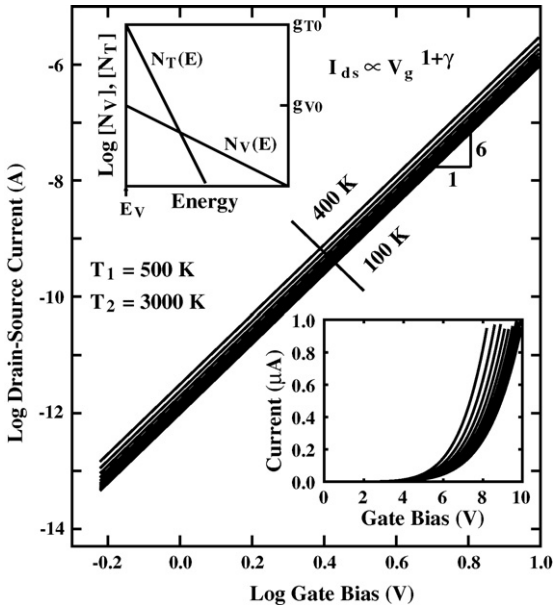

Fig. 12. Transfer curves for various temperatures in Log–Log scale (main plot) and linear scale (inset). For this simulation, $T_1 = 400$ K, $T_2 = 3000$ K and $\mu = 3\,\mathrm{cm}^2/\mathrm{Vs}$ (other parameters as in Table 1). A strongly bias-dependent mobility $\mu_{FET} \propto V_g^{\gamma}$ results, with $\gamma = 5$ independent of temperature. This is all the result of a DOS as indicated in the top inset; both the trap states as well as the conduction states exponetially distributed in energy with the Fermi level such that $N_T{}^+ \gg p$.

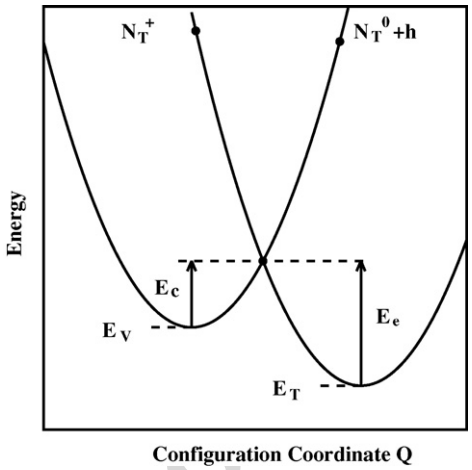

Fig. 13. Configuration-Coordinate Diagram. Upon capture of a carrier, the lattice can locally distort, represented by a generalized configuration coordinate Q, for instance the "breathing mode" of surrounding atoms. The system relaxes to a new local minimum. This demonstrates how the barriers for thermally activated capture (E_c) and emission (E_e) of carriers can be different and deviating from the trap depth $E_V - E_T$. The latter determines the final ratio of trapped and free charge, while the former two determine the speed at which this equilibrium is reached.

6. Transients

In the previous section, the bias dependence of the current and mobility was analyzed by taking into account localized states. It was there silently assumed that an equilibrium is achieved instantaneously upon changes of bias; any change of bias immediately causes a new distribution as calculated. This, however, is not an accurate picture. When the bias is changed, initial changes in charge density has necessarily to be of the free carrier kind, otherwise the charge would have no possibility to reach any given point in space. Holes, once injected into the valence band, become available for capture at the localized states. Under normal circumstances, the capture of carriers onto deep levels is fast and the emission thermally stimulated and slow [24]. When configurational distortions occur upon capture and release of charge, this picture can be modified. Both emission and capture become thermally activated, though with different activation energies, see Fig. 13. The capture of carriers can thus be expressed in the following equation

$$c_p(T) = c_{p0} T^2 \exp\left(\frac{-E_c}{kT}\right) \tag{36}$$

with c_{p0} the pre-factor and E_c the activation energy. For normal temperature ranges, the term T^2 can be considered constant. As demonstrated by Fig. 13, the activation energy is not necessarily the level depth found in the temperature scanned currents, $E_T - E_V$, see the Poole-Frenkel model of Eqs. (5) or (33).

Thus, a single, abundant deep level will cause a current exponentially decaying in time, with a characteristic time $\tau = 1/c_p$. When the levels receiving the charge are distributed in energy, a complicated convolution of capture processes can exist. Integration has to be done over all the levels that are available for receiving a free carrier. Each can have a different pre-factor. Many people have treated this in literature. Two results need to be highlighted. In the first model, originating from Kohlrausch in the 19th century [25], in glassy relaxations [26], the transients are of the stretched-exponential type

$$I_{ds} = I_0 \exp\left[-\left(\frac{t}{\tau}\right)^{\beta}\right] + I_\infty \tag{37}$$

with I_0 the starting current and I_∞ the final current, with the latter following the calculations given earlier. For very abundant traps, this current can be (close to) zero, as shown before. In another model, the currents follow a power-law [27]

$$I_{ds} = I_0 \left(\frac{t}{\tau}\right)^{-\alpha} \tag{38}$$

as a result of a multiple-trapping mechanism in an exponential DOS. It is often difficult to decide between the models on basis of experimental results.

7. Discussion and summary

In this second part of the modeling of TFTs, the effects of impurities are studied. In the first section, the effect of a field-dependent mobility is analyzed. In the Poole-Frenkel theory, the mobility depends on the field because adding a slanted potential offset lowers the barrier for escaping from a trap. As shown in the current work, this causes non-linearities in the I–V curves. These effects become more pronounced when the device dimensions are reduced. In standard MOS-FETs, short channel-effects are caused by overlapping depletion zones. In TFTs there are no depletion zones and short channel effects are exclusively caused by field dependence of the mobility.

The effects of doping of the semiconductor were considered with a focus on wide band-gap materials, such as most organic

semiconductors. The conclusions are that only traps cause a temperature dependent current (and thus a temperature-dependent mobility when defined via the derivative of the current as in Eq. (4) of Ref. [1]). When the traps are distributed in energy, the activation energy found in Arrhenius plots depend on the gate bias. This is called the Meyer-Neldel Rule which thus finds it's origin in abundant deep localized states.

In a previous work [28] we have shown that, using the theory of Shur and Hack [11], we were able to explain the Meyer-Neldel Rule. In the current work we arrive at a seemingly similar conclusion, but there is an important difference. Whereas Shur and Hack demonstrate a current depending on the gate bias

$$I_{ds} \propto V_g^{2T_2/T-1} \tag{39}$$

when the traps as well as the conduction states are distributed in space (parameters T_2 and T_1, respectively), we find a current with a different gate-bias dependence:

$$I_{ds} \propto V_g^{T_2/T} \tag{40}$$

Moreover, we find this only when exclusively the trap states are distributed in energy, with a normal conduction band. When both the trap states and the conduction states are distributed in energy, we find a current strongly, non-linearly depending on the bias dependent current, but the exponent in this power-law independent of temperature

$$I_{ds} \propto V_g^{T_2/T_1} \tag{41}$$

Another important difference is that we foresee an infinite iso-kinetic temperature for current, as shown in Fig. 10 , whereas Shur and Hack calculate the current to be bias-independent at a temperature $T = 2T_2$ (compare Eq. (39) with Eq. (40)). Both models predict a non-infinite iso-kinetic temperature for mobility equal to T_2, but our model needs only non-discrete trap states, while the Shur and Hack model needs distributed states for both the traps as well as the valence band. Finally, our theory can adequately describe situations in which the current is nearly independent on temperature, but strongly dependent on bias. This occurs when both conduction and trap states are distributed in energy. The experimental observation of such currents in earlier work [6] strengthens our theory.

The basic idea we should remain with, is that the measured mobility is an average over the trapped and delocalized states, and can take any value from zero up to the free charge value. Moreover, since the ratio of trapped-to-free charges depends on temperature, and bias, so does the measured mobility. In a recent work we have shown this model to be highly adequate for describing the conduction in FETs of sexithiophene (T6) [6].

The model including the traps is restricted to temperatures below T_2. This is because the integral for calculating the charged trap density (Eq. (24)) diverges when $T \geq T_2$. This, in turn, is caused by the assumption that the density of traps to spread over the entire energy range $-\infty$ to ∞ (Eq. (23)). This, is of course not a very realistic situation, but it simplifies the calculation, and since the contribution from states far away from the Fermi level is negligible, it is allowed. The biggest contribution to the integral comes from states in the vicinity of the Fermi level, as demonstrated by Fig. 8. It can therefore be said that the theory is qualitatively accurate for arbitrary distributions, as long as locally, at the Fermi level, the distribution decays exponentially and continues to do so for all voltages considered. Worth mentioning in this respect is the model of Fishchuk et al. [29] and similar models with states with Gaussian distributions. Such distributions are likely to also result in temperature and bias-dependent mobilities. Moreover, the model described by us will also do this for T beyond T_2, but before endeavoring these execute these calculations, more information about the DOS is needed.

In the section on transients we argued that the high density of traps can also causes transient effects. With a single trap level, the transients are exponential, but for other distributions of traps, the transients become non-exponential. This immediately establishes the link between non-exponential relaxations and the Meyer-Neldel rule, as also pointed out by Chen and Huang [30].

It is interesting to compare this to the work of Powell [31]. He explains the transients by a slow redistribution of charge in a direction (y) perpendicular to the direction (x) of current. Because of this redistribution, a new band bending is established and a different current results. In our model, no band bending exists, and the charges are only redistributed in energy. Free charge is trapped and becomes unavailable for external currents. While still contributing to the charge density, this charge does not contribute to current; a slowly decaying current is observed.

As to the location of the traps responsible for the described effects, it has to be mentioned that they are not necessarily inside the semiconductor material. It might be possible that the traps reside in the insulator. Experimentally, it is difficult to determine the exact location. Technologically, the issue might be addressed by trying a multitude of insulators, surface treatments, and active materials.

Finally, it has to be pointed out that in this work the density of traps is considered constant, and does not vary with bias, temperature, or time. It might be possible that this density is, for instance, changing over temperature. In previous works we have shown that at a temperature of 200 K the device shows abrupt changes in the conduction parameters [6]. This hints at a phase transition. Recently, we have shown that omnipresent water is responsible for this phase transition [32].

8. Final conclusions

A simple model was developed which can adequately predict the electrical characteristics of thin-film field-effect transistors, including intrinsic ambipolar devices. Moreover, it is argued that the model works equally well for accumulation FETs of any thickness; in the absence of localized states (donors) to store immobile positive charge, any induced charge is necessarily close to the interface.

First, the model was developed for trap-free devices. The model provides insight into the physical origin of the "contact effects", by showing clearly that the supra linear behavior of the current voltage characteristics could only be explained by introducing charge-carrier trap-states into the model, as explained in the second part. The filling of traps states also explains the appearance of a threshold voltage. The inclusion of a high density

of traps causes bias and temperature dependent mobility, including the Meyer-Neldel rule. We also show that if these states are distributed in energy, it will lead to non-exponential current transients, as normally observed.

Acknowledgement

This work has been financed by the Portuguese national Foundation of Science and Technology through project POCTI/FAT/47956/2002 and POSC research unit CEOT.

References

[1] P. Stallinga, H.L. Gomes, Synth. Met. 156 (2006) 1305.
[2] L.-L. Chua, J. Zaumseil, J.-F. Chang, E.C.-W. Ou, K.-H. Ho, H. Sirringhaus, R. Friend, Nature 434 (2005) 194.
[3] S.M. Sze, Physics of Semiconductor Devices, second ed., Wiley & Sons, New York, 1981 .
[4] G. Horowitz, Adv. Mat. 10 (1998) 365.
[5] S.V. Rakhmanova, E.M. Conwell, Appl. Phys. Lett. 76 (2000) 3822.
[6] P. Stallinga, J. Appl. Phys. 96 (2004) 5277.
[7] G. Horowitz, R. Hajlaoui, R. Bourguiga, M. Hajlaoui, Synth. Metals 101 (1999) 401.
[8] G. Horowitz, R. Hajlaoui, D. Fichou, A. El Kassmi, J. Appl. Phys. 85 (1999) 3202.
[9] G. Horowitz, M.E. Hajlaoui, R. Hajlaoui, J. Appl. Phys. 87 (2000) 4456.
[10] G. Horowitz, M.E. Hajlaoui, Adv. Mat. 12 (2000) 1046.
[11] M. Shur, M. Hack, J. Appl. Phys. 55 (1984) 3831.
[12] W. Meyer, H. Neldel, Z. Technol. 18 (1937) 588.
[13] E. Cantatore, E.J. Meijer, in: Proceedings of the 29th European Solid-State Circuits Conference (ESSCIRC '03), 2003, pp. 29–36.
[14] W. Bogusz, F. Krok, W. Piszczatowski, Solid State Ionics 119 (1999) 165.
[15] J.C. Wang, Y.F. Chen, Appl. Phys. Lett. 73 (1998) 948.
[16] E.J. Meijer, M. Matters, P.T. Herwig, D.M. de Leeuw, T.M. Klapwijk, Appl. Phys. Lett. 76 (2000) 3433.
[17] Y. Lubianiker, I. Balberg, J. Non-Cryst. Solids 227–230 (1998) 180.
[18] S.K. Ram, S. Kumar, R. Vanderhaghen, P. Roca i Cabarrocas, J. Non-Cryst. Solids 299–302 (2002) 411.
[19] M. Kondo, Y. Chida, A. Matsuda, J. Non-Cryst. Solids 198–200 (1996) 178.
[20] E.J. Meijer, D.B.A. Rep, D.M. de Leeuw, M. Matters, P.T. Herwig, T.M. Klapwijk, Synth. Metals 121 (2001) 1351.
[21] R.S. Crandall, Phys. Rev. B 43 (1991) 4057.
[22] K. Shimakawa, F. Abdel-Wahab, Appl. Phys. Lett. 70 (1997) 652.
[23] D.M. Goldie, J. Mater. Sci. 37 (2002) 3323.
[24] P. Blood, J.W. Orton, Techniques of Physics 14: The Electrical Characterization of Semiconductors: Majority Carriers and Electron States, Academic Press, 1992 .
[25] R. Kohlrausch in Rinteln, Ann. Phys. Chem. 72 (1847) 353 (in german).
[26] R.G. Palmer, D.L. Stein, E.A. Brahams, P.W. Anderson, Phys. Rev. Lett. 53 (1984) 958.
[27] M.R. Singh, Philos. Mag. 86 (2003) 797.
[28] P. Stallinga, H.L. Gomes, Org. El. 6 (2005) 137.
[29] I.I. Fishchuk, A.K. Kadashchuk, H. Bässler, D.S. Weiss, Phys. Rev. B 66 (2002) 205208.
[30] Y.F. Chen, S.F. Huang, Phys. Rev. B 44 (1991) 13775.
[31] M.J. Powell, IEEE Trans. Electron Dev. 36 (1989) 2753.
[32] H.L. Gomes, P. Stallinga, M. Cölle, D.M. de Leeuw, Appl. Phys. Lett. 88 (2006) 082101.